

Functional Clustering of the Human Inferior Parietal Lobule by Whole-Brain Connectivity Mapping of Resting-State Functional Magnetic Resonance Imaging Signals

Sheng Zhang¹ and Chiang-Shan R. Li¹⁻³

Abstract

The human inferior parietal lobule (IPL) comprised the lateral bank of the intraparietal sulcus, angular gyrus, and supramarginal gyrus, defined on the basis of anatomical landmarks and cytoarchitectural organization of neurons. However, it is not clear as to whether the three areas represent functional subregions within the IPL. For instance, imaging studies frequently identified clusters of activities that cut across areal boundaries. Here, we used resting-state functional magnetic resonance imaging (fMRI) data to examine how individual voxels within the IPL are best clustered according to their connectivity to the whole brain. The results identified a best estimate of seven clusters that are hierarchically arranged as the anterior, middle, and posterior subregions. The anterior, middle, and posterior IPL are each significantly connected to the somatomotor areas, superior/middle/inferior frontal gyri, and regions of the default mode network. This functional segregation is supported by recent cytoarchitectonics and tractography studies. IPL showed hemispheric differences in connectivity that accord with a predominantly left parietal role in tool use and language processing and a right parietal role in spatial attention and mathematical cognition. The functional clusters may also provide a more parsimonious and perhaps even accurate account of regional activations of the IPL during a variety of cognitive challenges, as reported in earlier fMRI studies.

Key words: angular gyrus; fMRI; inferior parietal lobule; intraparietal sulcus; resting-state functional connectivity; supramarginal gyrus

Introduction

AS A BRAIN AREA with heterogeneous functions, the human inferior parietal lobule (IPL) comprises the lateral bank of the intraparietal sulcus (IbIPS), angular gyrus (AG), and supramarginal gyrus (SMG)—which are defined on the basis of anatomical landmarks and cytoarchitectural organization of neurons as studied by the German anatomist Korbinian Brodmann (Garey, 2006; Tzourio-Mazoyer et al., 2002). The SMG and AG each corresponds to Brodmann area 39 and 40, and adjoins IbIPS, forming the IPL, as opposed to the superior parietal lobule, which is on the medial bank of the IPS. Numerous studies showed that each of these three subdivisions plays an important role in cognitive processes. For instance, the IbIPS has been implicated in visuo-spatial attention (Corbetta and Shulman, 2002; Egner

et al., 2008), motion perception (Claeys et al., 2003), visual memory (Xu and Chun, 2009), tool use (Ishibashi et al., 2011; Peeters et al., 2009), semantic processing (Chou et al., 2006a, 2006b), and mathematical cognition (Ansari, 2008; Cohen et al., 2000; Cohen Kadosh et al., 2007; Nieder and Dehaene, 2009; Piazza et al., 2007). The AG is involved in the memory of multiple sensory modalities (Cabeza et al., 2008; Hutchinson et al., 2009; Uncapher and Wagner, 2009), visual attention (Chambers et al., 2004), motion perception (Martinez-Trujillo et al., 2007), mathematical cognition (Dehaene et al., 2004; Delazer et al., 2003; Grabner et al., 2009), and language and semantic processing (Awad et al., 2007; Binder et al., 2009; Brownsett and Wise, 2010; Chou et al., 2006a, 2006b; Raposo et al., 2006; Sharp et al., 2010; Vigneau et al., 2006). Activations have been reported in the SMG in behavioral tasks that required visual attention

Departments of ¹Psychiatry and ²Neurobiology, Yale University, New Haven, Connecticut.
³Interdepartmental Neuroscience Program, Yale University, New Haven, Connecticut.

(Chambers et al., 2004; Stevens et al., 2005), working memory (Daselaar et al., 2004; Sommer et al., 2006; Uncapher and Wagner, 2009), motion perception (Martinez-Trujillo et al., 2007), and semantic processing (Raposo et al., 2006).

Altogether, the three regions appear to overlap functionally in multiple sensorimotor and cognitive domains, raising the possibility that these different perceptual and cognitive processes may selectively involve subregions of the IPL that can be functionally aggregated beyond the anatomical boundaries which define the lbIPS, AG, and SMG. For instance, the lbIPS, AG, and SMG were involved in memory encoding and retrieval (Clark and Wagner, 2003; Daselaar et al., 2004; Davachi et al., 2001; Otten and Rugg, 2001; Wagner and Davachi, 2001). However, these memory-related activities appear to concentrate at the boundaries of the lbIPS and AG (Clark and Wagner, 2003; Otten and Rugg, 2001), the lbIPS and SMG (Clark and Wagner, 2003; Wagner and Davachi, 2001), or the SMG and AG (Clark and Wagner, 2003; Daselaar et al., 2004; Otten and Rugg, 2001; Wagner and Davachi, 2001). Both lbIPS and AG were associated with semantic processing, but the activations were located at the boundary of the lbIPS and AG (Chou et al., 2006b). These findings suggest functional clusters that do not conform to the Brodmann demarcation of the IPL.

Indeed, recent studies accounting for topographical variability and using a quantitative, observer-independent definition of cytoarchitectonic borders showed that the IPS, SMG, and AG can each be divided into three, five, and two distinct subregions (Caspers et al., 2006, 2008; Choi et al., 2006; Scheperjans et al., 2008a, 2008b). Studies of white matter tractography based on diffusion-weighted imaging (DWI) (Mars et al., 2011; Wang et al., 2012) and those of functional clustering based on resting-state connectivity (Doucet et al., 2011; Nelson et al., 2010; Power et al., 2011; Yeo et al., 2011) also defined subregions that did not follow the boundaries of the IPS, AG, and SMG. However, none of these studies have systematically examined how these subregions are related to the IPS, AG, and SMG, as widely “localized” in functional neuroimaging.

Numerous studies have suggested connectivity analysis of resting-state functional magnetic resonance imaging (fMRI) data as a useful alternative to characterize functional subdivisions of a brain region. This approach parceled brain areas on the basis that each subregion has a unique pattern of connectivities—a “functional fingerprint” (Passingham et al., 2002). Specifically, low-frequency blood oxygenation level-dependent (BOLD) signal fluctuations reflect connectivity between functionally related brain regions (Biswal et al., 1995; Fair et al., 2007; Fox and Raichle, 2007). Studies of this “spontaneous” activity have provided insights into the intrinsic functional architecture of the brain and shown that the spontaneous fluctuations are present in many neuro-anatomical systems, including motor, visual, auditory, default mode, memory, language, dorsal attention, and ventral attention systems (Fox and Raichle, 2007). Based on the findings that regions with similar functionality tend to be correlated in their spontaneous BOLD activity, investigators described subareal boundaries for the thalamus (Zhang et al., 2008, 2010), basal ganglia (Barnes et al., 2010), medial superior frontal cortex (Kim et al., 2010; Zhang et al., 2012a), anterior cingulate cortex (Margulies

et al., 2007), orbitofrontal cortex (Kahnt et al., 2012), cerebellum (O’Reilly et al., 2010), and precuneus (Cauda et al., 2010; Margulies et al., 2009; Zhang and Li, 2012).

Here, we examined the functional subdivisions of the IPL by employing a voxelwise approach and clustering individual voxels according to their “functional fingerprint” or pattern of connectivity to the entire brain. We have three specific aims. First, we investigated functional subdivisions of the entire IPL by characterizing both cortical and subcortical connectivities of a large resting-state fMRI data set. In particular, previous studies suggested the AG to be a part of the default mode network or DMN (Buckner et al., 2008; Fox et al., 2005; Greicius et al., 2003; Raichle et al., 2001). Since this brain region harbors heterogeneous functions, we examined which part of the AG belongs to the DMN. Second, we examined the differences in regional connectivities and highlighted the opposing pattern of connectivities between the identified IPL subdivisions. Third, a previous work on connectivity-based IPL parcellation did not examine hemispheric differences. We, thus, explored hemispheric differences in IPL connectivity given their importance in parietal functioning. We hope that the new data will facilitate future studies of IPL functions.

Materials and Methods

Resting-state data

A total of 225 healthy subjects’ resting-state fMRI data were pooled from three datasets (Leiden_2180/Leiden_2200, Newark, and Beijing_Zang, $n=144$) downloadable from the 1000 Functional Connectomes Project (Biswal et al., 2010) and our laboratory ($n=81$). Data was recorded as one scan per participant under 3-T magnet with 18–53 (mean=24) years of age, 109 men, duration: 4.5–10 min and eyes closed during scans (Table 1). Individual subjects’ images were viewed one by one to ensure that the whole brain was covered.

Imaging data preprocessing

Brain imaging data were preprocessed using Statistical Parametric Mapping (SPM 8; Wellcome Department of Imaging Neuroscience, University College London, United Kingdom), as described in our previous work (Zhang et al., 2012a; Zhang and Li, 2012). Briefly, images of each individual subject were first realigned (motion corrected) and corrected for slice timing. Individual structural image was normalized to a Montreal Neurological Institute (MNI) echo-planar imaging template with affine registration followed by nonlinear transformation (Ashburner and Friston, 1999; Friston et al., 1995). The normalization parameters determined for the structural volume were then applied to the corresponding functional image volumes for each subject. Finally, the images were smoothed with a Gaussian kernel of 8 mm at Full Width at Half Maximum.

Additional preprocessing was applied to reduce spurious BOLD variances that were unlikely to reflect neuronal activity (Fair et al., 2007; Fox et al., 2005; Fox and Raichle, 2007; Rombouts et al., 2003). The sources of spurious variance were removed through linear regression by including the signal from the ventricular system, the white matter, and the whole brain, in addition to the six parameters obtained by rigid body head motion correction. First-order derivatives

TABLE 1. DEMOGRAPHIC DATA AND IMAGING PARAMETERS FOR THE RESTING-STATE FUNCTIONAL MAGNETIC RESONANCE IMAGING DATASETS SELECTED FROM THE IMAGE REPOSITORY FOR THE 1000 FUNCTIONAL CONNECTOMES PROJECT AND OUR OWN DATASET

Dataset	Subjects	Ages (years)	Timepoints	TR (s)	Slice acquisition order
Beijing_Zang	31 M/66 F	18–26	225	2	Interleaved ascending
Leiden_2180	10 M/0 F	20–27	215	2.18	Sequential descending
Leiden_2200	11 M/8 F	18–28	215	2.2	Sequential descending
Newark	9 M/9 F	21–39	135	2	Interleaved ascending
Our own	48 M/33 F	19–53	295	2	Interleaved ascending

M, males; F, females; TR, repetition time.

of the whole brain, ventricular, and white matter signals were also included in the regression.

Cordes and colleagues suggested that BOLD fluctuations below a frequency of 0.1 Hz contribute to regionally specific BOLD correlations (Cordes et al., 2001). The majority of resting-state studies low-pass filtered BOLD signal at a cut-off of 0.08 or 0.1 Hz (Fox and Raichle, 2007). Thus, we applied a temporal band-pass filter ($0.009 \text{ Hz} < f < 0.08 \text{ Hz}$) to the time course in order to obtain low-frequency fluctuations (Fair et al., 2007; Fox et al., 2005; Fox and Raichle, 2007; Lowe et al., 1998).

Linear correlations with 116 anatomical masks

We used the anatomical parcellation algorithm to delineate 116 automated anatomical labeling (AAL) masks from the MNI template (Tzourio-Mazoyer et al., 2002). Each of the BOLD time courses was averaged spatially for all 116 seed regions. We computed the correlation coefficient between the average time course of each mask and the time courses of each of the individual voxels of the IPL for individual subjects.

To assess and compare the resting-state “correlograms,” we converted these image maps, which were not normally distributed, to z score maps by Fisher’s z transform (Berry and Mielke, 2000; Charles et al., 2004; Jenkins and Watts, 1968): $z = 0.5 \log_e [(1+r)/(1-r)]$. The z maps were used in group, random-effect analyses (Penny et al., 2004). A one-sample t -test was applied to the “ z maps” across 225 subjects for each of the 116 correlograms for a further analysis.

Parcelation of the IPL based on functional connectivity

Voxels within the entire IPL, defined by combining masks of the lbIPS, AG, and SMG from an MNI template created by Tzourio-Mazoyer et al. (2002), were subject to functional connectivity-based segmentation, with each voxel represented by 116 t values. A K-means algorithm was applied to cluster the voxels within the IPL on the bases of the 116 t values.

As an unsupervised learning algorithm, K-means clustering classifies a given data set into an a-priori set of K clusters by minimizing an objective squared error function as shown in Equation (1):

$$J = \sum_{j=1}^k \sum_{i=1}^n \left\| X_i^{(j)} - c_j \right\|^2 \quad (1)$$

where $\|x_i^{(j)} - c_j\|^2$ is a distance measure between a data point $x_i^{(j)}$ and the cluster center c_j (MacQueen, 1967). The algorithm was executed by:

1. Placing K points into the space represented by the objects that are being clustered. These points represent initial group centroids.
2. Assigning each object to the group that has the closest centroid.

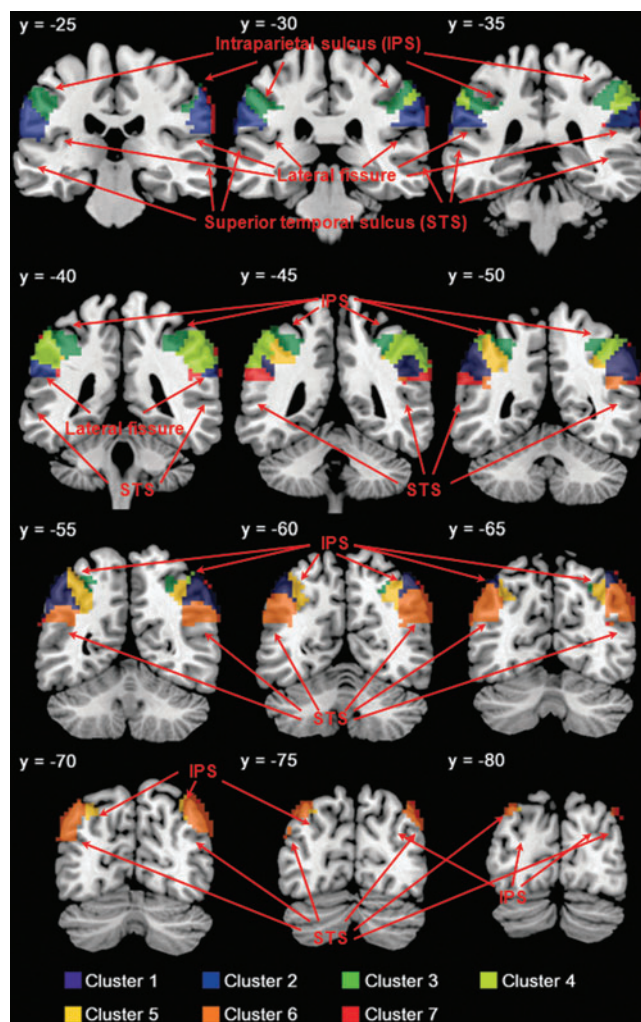
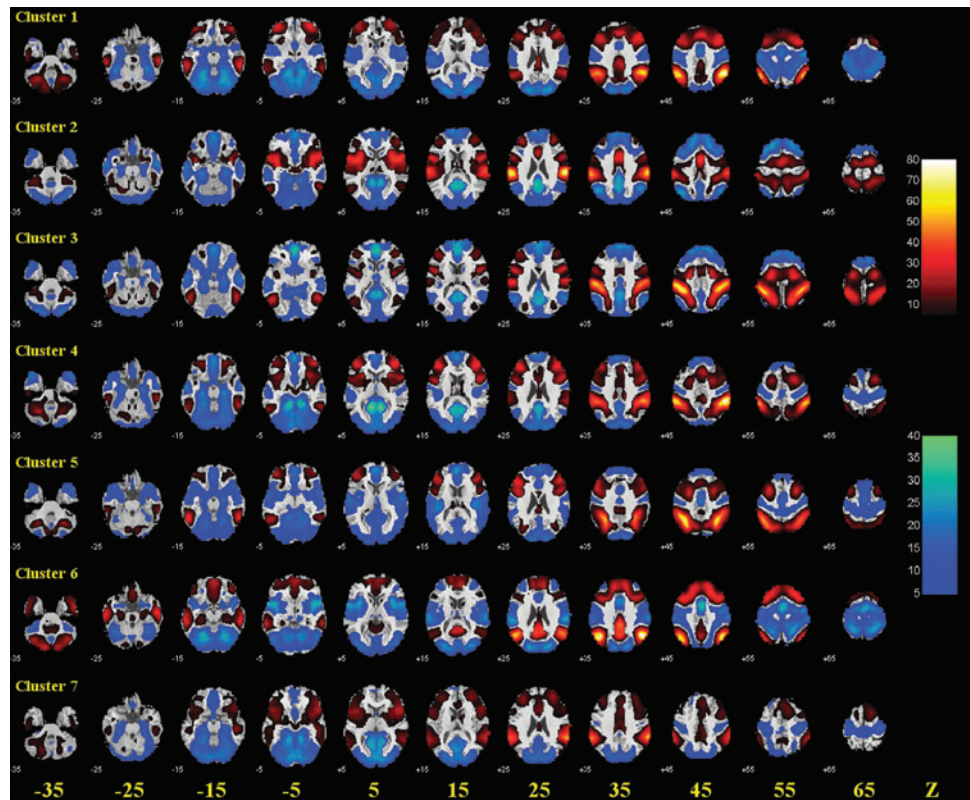


FIG. 1. K-means clustering of functional connectivities of individual voxels segments in the inferior parietal lobule (IPL) to seven clusters. Clusters are in different colors and overlaid on a T1 structural image in coronal slices at $y = -25, -30, -35, -40, -45, -50, -55, -60, -65, -70, -75, -80$ mm.

FIG. 2. Group results of voxel-wise functional connectivity of each of the seven clusters of the IPL. Positive (warm color) and negative (cold color) correlations were superimposed on axial slices at $Z = -35, -25, -15, -5, 5, 15, 25, 35, 45, 55, 65$ mm of a structural image. $n = 225$, $p < 0.05$, corrected for family-wise error or family-wise error of multiple comparisons. Color scales reflect T values of one-sample t test.



3. When all objects have been assigned, recalculating the positions of the K centroids.
4. Repeating Steps 2 and 3 until the centroids no longer move. This produces a separation of the objects into groups from which the metric to be minimized can be calculated.

In order to determine the optimal number of clusters that best described the data set, we used the Bayesian Information Criterion (BIC) (Gentle et al., 2004; Schwarz, 1978), which is widely used for model identification in time series and linear regression:

$$BIC = n \ln \left(\frac{RSS}{n} \right) + k \ln(n) \quad (2)$$

where n is the number of observations; k is the number of the class; and RSS is the residual sum of squares from the K-means model. Given any two clustering number k s, the one with a lower BIC value was preferred. Further, since the K-means algorithm is sensitive to the initial, randomly selected cluster centers, we repeated this algorithm 1000 times to alleviate the effect of the initial conditions.

Results

The results of 1000 runs of K-means clustering suggested an optimal cluster number of seven according to the BIC (Supplementary Fig. S1a; Supplementary Data are available online at www.liebertpub.com/brain). Figures 1 and 2 each shows the seven clusters and t statistic connectivity map of individual clusters.

To examine the relationship of the seven clusters identified from K-means clustering, we applied hierarchical clus-

tering to their connectivity maps (see Supplementary Methods for details). The results showed that the seven clusters were broadly divided into the anterior (clusters 2, 3), middle (cluster 1, 4, 5, 7), and posterior (clusters 6) IPL (Supplementary Fig. S1b). We, thus, re-ran K-means clustering for a three-cluster solution. The results confirmed segmentation of the IPL into anterior, middle, and posterior subdivisions (Fig. 3). Figure 3 contrasts the areal boundaries of the three clusters as combined from seven subclusters, the three clusters identified directly from K-means clustering, and the lbIPS, SMG, and AG masks from the AAL atlas.

The anterior IPL (clusters 2 and 3)

The anterior IPL comprised the dorsal-anterior IPL (cluster 3, 75% voxels from the lbIPS, 23% voxels from the SMG, and 2% voxels from the AG) and the ventral-anterior IPL (cluster 2, 100% voxels from the SMG) (Fig. 1; Table 2).

The anterior IPL (both clusters 2 and 3) showed positive connectivity with the primary motor cortex, bilateral opercular and left triangular part of the inferior frontal gyri, rolandic operculum, supplementary motor area, insula, postcentral gyrus, superior parietal lobule, as well as left cerebellar lobules, and negative connectivity with the middle and medial parts of the orbital frontal gyri, left olfactory bulb, medial superior frontal gyrus, gyrus rectus, posterior cingulate gyrus, parahippocampus, calcarine sulcus, cuneus, fusiform gyrus, precuneus, as well as cerebellar lobules III, IV, V, and vermis lobules III, IV, V (Schmahmann et al., 1999, 2000) (Fig. 2 and Supplementary Table S1).

The anterior IPL also showed positive connectivity with the middle frontal gyrus, left inferior occipital gyrus, left paracentral gyrus, and right cerebellar lobules (dorsal-anterior IPL; cluster 3), and with the right triangular part of the

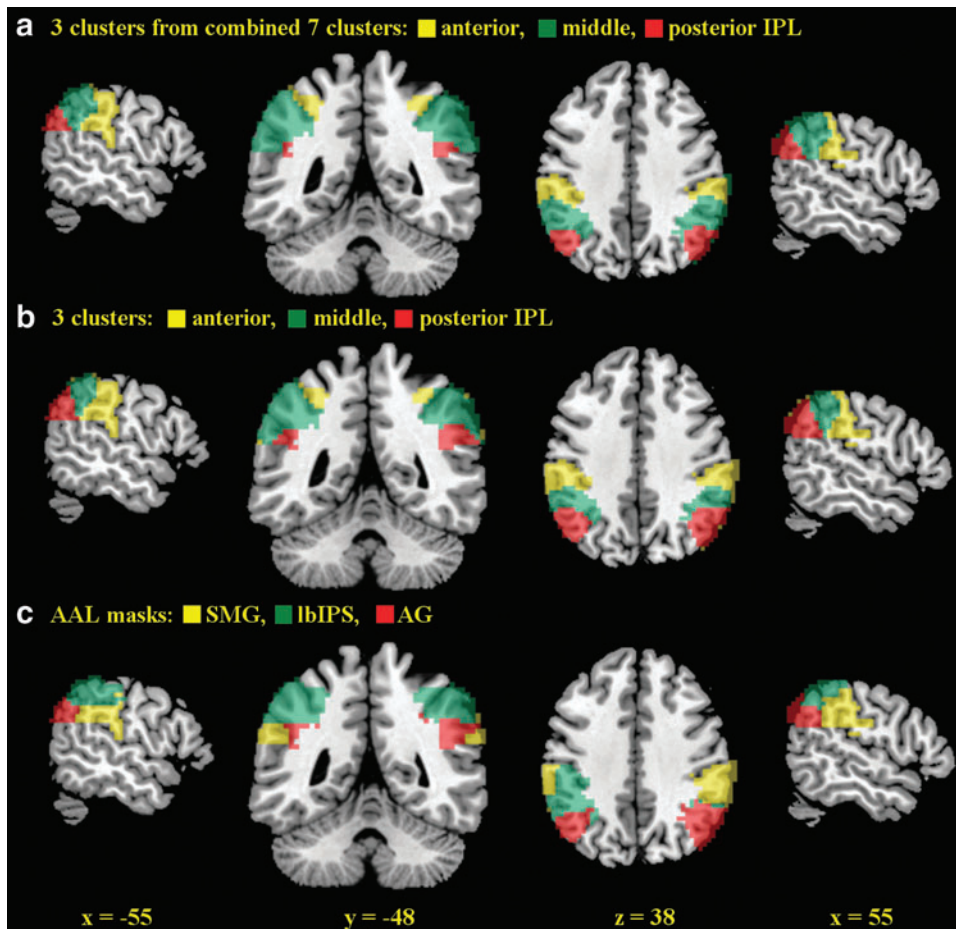


FIG. 3. Comparison between (a) three subregions of the IPL as combined from individual subclusters in the seven-cluster solution; (b) three subregions of the IPL from a three-cluster solution with K-mean clustering; and (c) lateral bank of the intraparietal sulcus (lbIPS), supramarginal gyrus (SMG), and angular gyrus (AG) clusters from AAL masks (Tzourio-Mazoyer et al., 2002).

inferior frontal gyrus, orbital part of the inferior frontal gyrus, middle cingulate gyrus, amygdala, right paracentral gyrus, putamen, pallidum, thalamus, Heschl's gyrus, superior temporal gyrus/pole, and right middle temporal pole (ventral-anterior IPL; cluster 2); and negative connectivity with the right olfactory bulb, anterior cingulate gyrus,

amygdala, right middle temporal gyrus, and left middle temporal pole (dorsal-anterior IPL; cluster 3), and with the superior, middle, and inferior occipital gyri, and left cerebellar lobule VI (ventral-anterior IPL; cluster 2) These results are shown in Figure 2 and summarized in Supplementary Table S1.

TABLE 2. VOLUME PERCENTAGES OF EACH OF THE SEVEN INFERIOR PARIETAL LOBULE CLUSTERS

Clusters	lbIPS		SMG		AG	
	A%	B%	A%	B%	A%	B%
Anterior IPL	32	40	62	58	1	2
Dorsal-anterior IPL (cluster 3)	32	75	12	23	1	2
Ventral-anterior IPL (cluster 2)	0	0	50	100	0	0
Middle IPL	64	50	37	27	30	23
Dorsal anterior-middle IPL (cluster 4)	23	60	18	40	0	0
Ventral anterior-middle IPL (cluster 7)	1	8	13	79	2	13
Lateral posterior-middle IPL (cluster 1)	21	57	6	13	15	30
Medial posterior-middle IPL (cluster 5)	19	67	0	0	13	33
Posterior IPL	4	7	1	1	69	92
Posterior IPL (cluster 6)	4	7	1	1	69	92

$A\% = V_{ij}/V_j$ and $B\% = V_{ij}/V_i$, where i = our cluster 1, 2, ..., 7; j = lbIPS, SMG, and AG; V_{ij} is the number of voxels from the intersection of our cluster i and lbIPS/SMG/AG; V_i is the number of voxels from our cluster i ; and V_j is the number of voxels from lbIPS/SMG/AG.

$A\%$, the volume percentage of the cluster relative to the lbIPS/SMG/AG; $B\%$, the volume percentage of voxels within the lbIPS/SMG/AG relative to the whole cluster.

IPL, inferior parietal lobule; lbIPS, intraparietal sulcus; SMG, supramarginal gyrus; AG, angular gyrus.

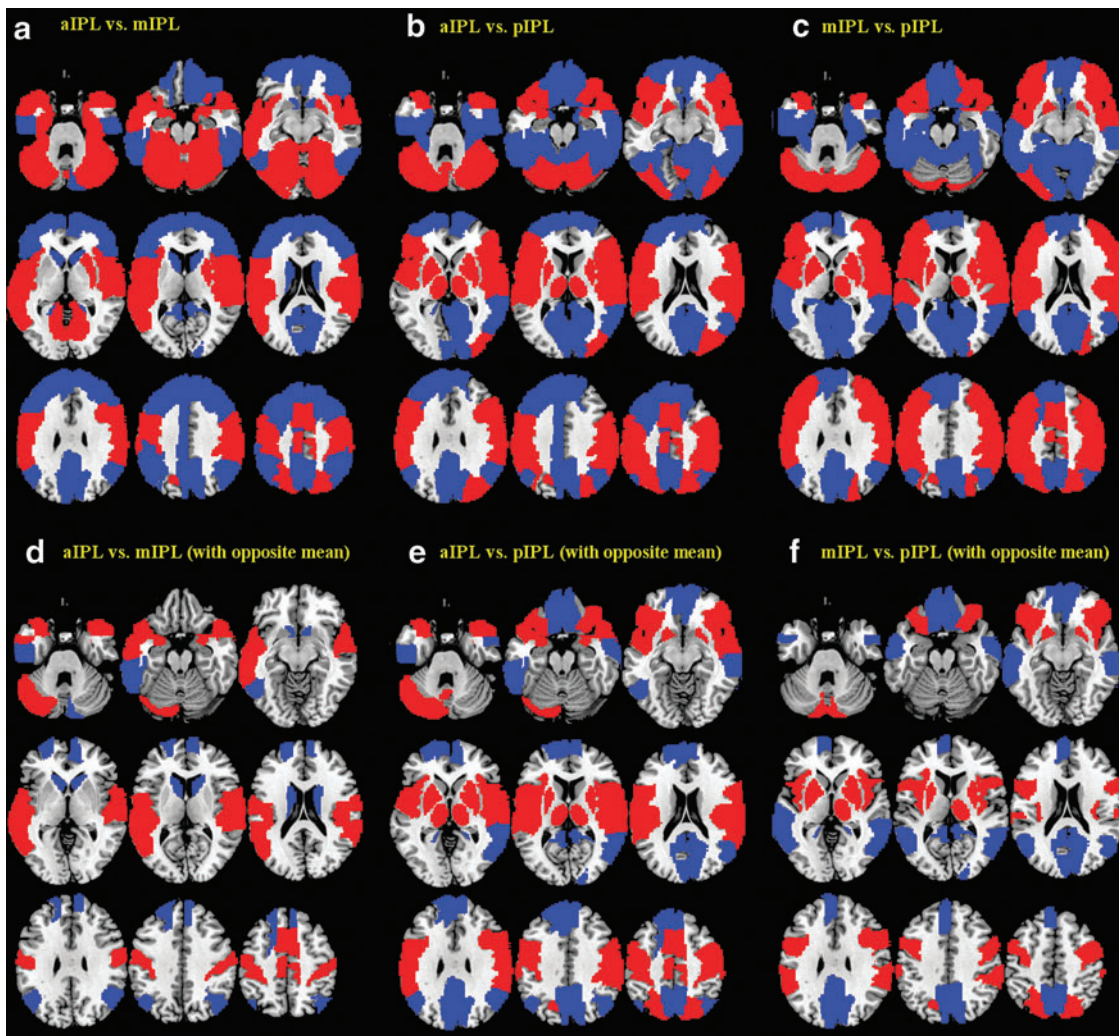


FIG. 4. Differences in functional connectivity between anterior (a), middle (m), and posterior (p) IPL [(a–c), upper row]. Connectivities with each of the 116 AAL masks was examined pairwise with paired t tests. Results at $p < 0.00014$ ($p < 0.05$, corrected for multiple comparisons) are superimposed on axial slices at $Z = -30, -20, -10, 0, 10, 20, 30, 40, 50$ mm of a structural image. Red: aIPL > mIPL (a), aIPL > pIPL (b), and mIPL > pIPL (c); blue: aIPL > mIPL, aIPL > pIPL, and mIPL > pIPL. [(d–f), bottom row] Significant differences are shown only for regions with an opposite pattern of connectivity between aIPL and mIPL (d), aIPL and pIPL (e), and mIPL and pIPL (f). See Supplementary Tables S2–S4 for additional information.

The middle IPL (clusters 1, 4, 5, and 7)

The middle IPL comprised the dorsal anterior-middle IPL (cluster 4, 60% voxels from the lbIPS and 40% voxels from the SMG), ventral anterior-middle IPL (cluster 7, 79% voxels from the SMG, 13% voxels from the AG, and 8% voxels from the lbIPS), lateral posterior-middle IPL (cluster 1, 57% voxels from the lbIPS, 30% voxels from the AG, and 13% voxels from the SMG), and medial posterior-middle IPL (cluster 5, 67% voxels from the lbIPS, and 33% voxels from the AG) (Fig. 1; Table 2).

The middle IPL (clusters 1, 4, 5, and 7) showed positive connectivity with the middle frontal gyrus and triangular part of the inferior frontal gyrus, and negative connectivity with the olfactory bulb, parahippocampus, calcarine, cuneus, right inferior occipital gyrus, fusiform, as well as cerebellar crus I, cerebellar lobules III, IV, V, VI, and ver-

mis lobules III, IV, V, VI, VII (Fig. 2 and Supplementary Table S1).

Other than these connectivities shared by all four clusters of the middle IPL, the anterior-middle IPL (cluster 4 and 7) also showed positive connectivity with the right superior frontal gyrus, opercular part of the inferior frontal gyrus, orbital part of the inferior frontal gyrus, insula, middle cingulate gyrus, putamen, pallidum, and right superior temporal pole, and negative connectivity with the left medial part of the orbital frontal gyrus, gyrus rectus, posterior cingulate gyrus, superior and middle occipital gyri, left inferior occipital gyrus, and cerebellar lobule X. The posterior-middle IPL (cluster 1 and 5) showed positive connectivity with the lateral part of the orbital frontal gyrus and right posterior cingulate gyrus, and negative connectivity with the rolandic operculum, supplementary motor area, amygdala, paracentral gyrus, Heschl's gyrus, superior temporal gyrus, right

TABLE 3. DIFFERENCES IN FUNCTIONAL CONNECTIVITY ($p < 0.00014$, or $p < 0.05$, CORRECTED FOR MULTIPLE COMPARISONS) BETWEEN THE ANTERIOR AND MIDDLE (aIPL Vs. mIPL), BETWEEN ANTERIOR AND POSTERIOR (aIPL Vs. pIPL), AND BETWEEN MIDDLE AND POSTERIOR IPL (mIPL Vs. pIPL)

	<i>aIPL vs. mIPL</i>	<i>aIPL vs. pIPL</i>	<i>mIPL vs. pIPL</i>
Bilateral primary motor cortex		>	>
Left superior frontal gyrus	<	<	
Bilateral middle part of orbital frontal gyrus		<	<
Bilateral opercular part of inferior frontal gyrus		>	>
Bilateral orbital part of inferior frontal gyrus		>	>
Bilateral rolandic operculum	>	>	
Bilateral supplementary motor area	>	>	
Left medial superior frontal gyrus		<	<
Right medial superior frontal gyrus	<	<	
Bilateral medial part of orbital frontal gyrus		<	<
Bilateral gyrus rectus		<	<
Bilateral insula		>	>
Bilateral posterior cingulate gyrus		<	<
Bilateral amygdala	>	>	
Bilateral cuneus		<	<
Bilateral postercentral gyrus	>	>	
Bilateral superior parietal lobule		>	>
Bilateral precuneus		<	<
Bilateral paracentral gyrus	>	>	
Bilateral caudate	<		
Bilateral putamen		>	>
Bilateral pallidum		>	>
Left thalamus		>	
Right thalamus		>	>
Bilateral Heschl's gyrus	>	>	
Bilateral superior temporal gyrus and pole	>	>	
Right middle temporal gyrus		<	<
Right middle temporal pole	>	>	
Left inferior temporal gyrus	<	<	
Left cerebellum crus part 1	>	>	
Left cerebellum crus part 2		>	
Right cerebellum crus part 2	<		<
Left cerebellum part 7b		>	>
Left cerebellum part 8		>	>
Right cerebellum part 9		<	
Vermis part 9		>	

Only brain regions showing an opposite pattern of connectivity between the two respective clusters are shown here. “>” indicates aIPL > mIPL, aIPL > pIPL, or mIPL > pIPL, and “<” indicates aIPL < mIPL, aIPL < pIPL, or mIPL < pIPL.

superior temporal pole, and middle temporal pole (Fig. 2 and Supplementary Table S1).

Positive connectivity was further observed between the dorsal anterior-middle IPL (cluster 4) and the left primary motor cortex, right middle frontal gyrus, lateral part of the orbital frontal gyrus, superior parietal lobule, and cerebellar lobules VIIb, VIII; between the ventral anterior-middle IPL (cluster 7) and the supplementary motor area, medial superior frontal gyrus, anterior cingulate gyrus, superior and middle temporal gyri, and left superior temporal pole; between the lateral posterior-middle IPL (cluster 1) and the superior frontal gyrus, right middle part of the orbital frontal gyrus, right orbital part of the inferior frontal gyrus, medial superior frontal gyrus, right anterior, middle, and left posterior cingulate gyrus, right precuneus, and right caudate; and between the medial posterior-middle IPL (cluster 5) and the left primary motor cortex, opercular part of the inferior frontal gyrus, superior parietal lobule, and right cerebellar crus II and cerebellar lobule VIIb (Fig. 2 and Supplementary Table S1).

Negative connectivity was further observed between the dorsal anterior-middle IPL (cluster 4) and the left middle part of the orbital frontal gyrus, right medial part of the orbital frontal gyrus, precuneus, and Heschl's gyrus; between the lateral posterior-middle IPL (cluster 1) and the right primary motor cortex, superior, middle, and left inferior occipital gyri, postcentral gyrus, as well as cerebellar lobule X and vermis lobules I, II; and between the medial posterior-middle IPL (cluster 5) and the medial superior frontal gyrus, medial part of the orbital frontal gyrus, gyrus rectus, insula, anterior cingulate gyrus, left superior temporal pole, and middle temporal gyrus (Fig. 2 and Supplementary Table S1).

The posterior IPL (clusters 6)

The posterior IPL comprised cluster 6 (92% voxels from the AG, 7% voxels from the lbIPS, and 1% voxels from the SMG) (Fig. 1; Table 2). The posterior IPL showed positive connectivity with the superior and middle frontal gyri,

TABLE 4. DIFFERENCES IN FUNCTIONAL CONNECTIVITY BETWEEN LEFT- AND RIGHT-HEMISPHERIC INFERIOR PARIETAL LOBULE CLUSTERS

	Cluster 1		Cluster 2		Cluster 3		Cluster 4		Cluster 5		Cluster 6		Cluster 7	
	L	R	L	R	L	R	L	R	L	R	L	R	L	R
Left primary motor cortex							+							
Right superior frontal G								+						
Right middle frontal G					+									
Right triangular part of inferior frontal G					+									
Left orbital part of inferior frontal G										-	+			
Right orbital part of inferior frontal G									+					
Right insula									+					
Right middle cingulate G									+					
Right precuneus		-												
Right putamen									+					
Left Heschl's G						-								+
Right Heschl's G														+
Left cerebellum crus part 1									+					
Right cerebellum crus part 1		+								+				-
Left cerebellum crus part 2									+					
Right cerebellum part 6									-					

Voxel-wise connectivities were averaged for each of the 116 AAL masks. Significant connectivities at a threshold of $p < 0.05$, corrected for family-wise error or FWE of multiple comparisons, were marked by “+” (positive) and “-” (negative). Only brain regions showing an opposite pattern of connectivity between the left- and right hemispheric clusters are shown here.

L, left; R, right; G, gyrus; AAL, automated anatomical labeling.

middle and medial parts of the orbital frontal gyri, medial superior frontal gyrus, gyrus rectus, posterior and left middle cingulate gyri, precuneus, inferior temporal gyrus, and right cerebellar lobule IX, and negative connectivity with the primary motor cortex, opercular and orbital parts of the inferior frontal gyri, rolandic operculum, supplementary motor area, insula, amygdala, superior, middle, and inferior occipital gyri, postcentral and paracentral gyri, superior parietal lobule, putamen, right pallidum, Heschl's gyrus, superior temporal gyrus, superior and middle temporal poles, as well as cerebellar crus I, right cerebellar crus II, cerebellar lobule VI, and vermis lobules VI, VII.

Notably, all seven IPL clusters showed negative connectivity with the lingual gyri, and none showed connectivity with the hippocampus, left caudate, right inferior temporal gyrus, left cerebellar lobule IX, and vermis lobules VIII, IX, and X (Fig. 2 and Supplementary Table S1).

Differences in functional connectivity between the IPL subdivisions

We quantified the differences in functional connectivity of the anterior, middle, and posterior IPL. To better represent the results, we separated the whole brain into 116 regions based on the AAL atlas and examined the differences in functional connectivity with each region with paired t tests across the entire cohort of subjects. Results were summarized in Supplementary Tables S2–S4. Later, we described those brain regions showing not only significant differences but also an opposite pattern of connectivity between the three IPL subdivisions (Fig. 4d–f; Table 3).

Compared with both the middle and posterior IPL, the anterior IPL showed greater functional connectivity with the rolandic operculum, supplementary motor area, amygdala, postcentral and paracentral gyri, Heschl's gyrus, superior temporal gyrus and pole, right middle temporal pole, and cer-

ebellar crus I, as well as less connectivity with the left superior frontal gyrus, right medial superior frontal gyrus, and left inferior temporal gyrus. Compared with the posterior IPL, both anterior and middle IPL showed greater connectivity with the primary motor cortex, opercular and orbital parts of the inferior frontal gyrus, insula, superior parietal lobule, putamen, pallidum, right thalamus, as well as left cerebellar crus II and left cerebellar lobules VIIIb and VIII. Conversely, compared with the anterior and middle IPL, the posterior IPL showed greater connectivity with the middle and medial parts of the orbital frontal gyrus, left medial superior frontal gyrus, gyrus rectus, posterior cingulate gyrus, cuneus, precuneus, and middle temporal gyrus. Compared with the anterior IPL, the middle IPL showed greater connectivity with the caudate and right cerebellar crus II. Compared with the posterior IPL, the anterior IPL showed greater connectivity with the left thalamus and vermis lobule IX, as well as less connectivity with the right cerebellar lobule IX. Compared with the middle IPL, the posterior IPL showed greater connectivity with the right cerebellar crus II.

Hemispheric differences in IPL connectivity

We examined the differences in functional connectivity between the left and right IPL. First, voxels within the left and right IPL mask were subject to functional connectivity-based segmentation separately, with each voxel represented by 116 t values. The resulting clusters were very similar to those obtained with the entire IPL (Supplementary Fig. S2). Second, we compared the functional connectivity of the left and right clusters with the 116 AAL regions. Since regions usually showed higher connectivity to a seed region within the same than a different hemisphere, a direct comparison would only highlight these hemispheric differences. We, thus, focused on those brain regions showing significant connectivity with one hemispheric but not the other cluster,

Subdivisions of the IPL

Based on cytoarchitectonic maps, previous studies suggested that the IPL can be divided into subregions beyond the lbIPS, SMG, and AG (Caspers et al., 2006, 2008; Choi et al., 2006). The IPS was subdivided into the human intraparietal area 2 (hIP2), occupying anterior and lateral IPS; the human intraparietal area 3, occupying posterior IPS; and the human intraparietal area 1, located immediately posterior and medial to hIP2 (Choi et al., 2006; Scheperjans et al., 2008a, 2008b). The SMG was divided into three larger and dorsal subregions, PFm, PF, and PFt, and two smaller and ventral subregions, PFcm and PFop (Caspers et al., 2006, 2008). Finally, the AG consists of the anterior and posterior areas PGa and PGp, respectively (Caspers et al., 2006, 2008). More recently, two studies employed DWI tractography to segment right and left IPL (Mars et al., 2011; Wang et al., 2012). The right-hemispheric IPL was divided into five subregions: the most anterior cluster (red, color coded as in Fig. 2 of Mars et al., 2011); two clusters (blue and green) located directly posterior to the red cluster; one cluster (magenta) located posterior to blue and green clusters and occupying the anterior AG; and the most posterior cluster (yellow) that occupies the posterior AG (Mars et al., 2011). The left-hemispheric IPL was divided into six subclusters: a dorsal anterior cluster (blue, color coded as in Fig. 1 of Wang et al., 2012); a ventral anterior cluster (green); and four clusters successively posterior to the green cluster: light green, yellow, orange, and red. The yellow cluster occupies the most posterior part of the SMG, and the orange and red cluster each corresponds to the anterior and posterior AG, respectively (Wang et al., 2012). We compared our clustering results with these previous findings in Table 5.

Thus, analyses of resting-state connectivity suggest distinct functional clusters in the IPL that do not correspond to the anatomical boundaries of lbIPS, SMG, and AG. These functional clusters are also evident from many imaging studies of cognitive tasks. For instance, Otten and Rugg (2001) showed that activations in the lbIPS ($x = -54$, $y = -42$, $z = 48$), SMG ($x = 63$, $y = -45$, $z = 27$), and AG ($x = -54$, $y = -54$, $z = 36$) during memory encoding were related to retrieval performance, suggesting that the entire IPL is involved in this mnemonic process. On the other hand, all the coordinates of the peak activations were within the mid-

dle IPL cluster as identified here. Similarly, responses to remembered versus forgotten items in two clusters each within the lbIPS ($x = 49$, $y = -49$, $z = 48$) and SMG ($x = 60$, $y = -43$, $z = 30$) could be localized to the middle IPL cluster (Daselaar et al., 2004). Studies of semantic processing as in contrasting related versus unrelated word pair identified activations in the lbIPS ($x = -36$, $y = -62$, $z = 50$) and AG ($x = 36$, $y = -62$, $z = 45$), both of which are within the middle IPL (Chou et al., 2006b). Furthermore, an observation of tool use led to activations in the lbIPS ($x = -42$, $y = -42$, $z = 56$) and SMG ($x = -52$, $y = -26$, $z = 34$), both of which are within the anterior IPL (Peeters et al., 2009). A few other studies have similarly demonstrated functional activations that are best localized to the IPL clusters as identified here with whole-brain connectivity analysis (Clark and Wagner, 2003; Davachi et al., 2001; Mayer et al., 2006; Wagner and Davachi, 2001).

Functional roles of the anterior, middle, and posterior IPL

The anterior IPL (cluster 2 and 3) showed significant connectivity with the primary motor cortex, postcentral and paracentral gyri, and supplementary motor area, consistent with a role in sensorimotor processing (Claeys et al., 2003; Ishibashi et al., 2011; Martinez-Trujillo et al., 2007; Peeters et al., 2009). In contrast, the middle IPL (cluster 1, 4, 5, and 7) showed connectivity with the lateral frontal regions but not with the somatic motor areas. Claeys and colleagues hypothesized a lower-level, luminance-based and a higher-level, attention-based system for motion processing, each involving a region (Claeys et al., 2003) that corresponds to the anterior and middle IPL cluster. Thus, the anterior IPL, directly connected with the somatic motor areas, and the middle IPL, connected with lateral frontal regions, may play a specific role each in luminance-based and attention-based motion processing. These findings were also consistent with diffusion tensor imaging tractography showing a high probability of connection of the ventral premotor cortex with the anterior but not middle or posterior IPL (Rushworth et al., 2006).

The posterior IPL showed positive connectivity with regions of the DMN, including medial prefrontal cortex, posterior cingulate cortex, and precuneus, and negative connectivity with regions of the task-related network such as somatomotor areas (Buckner et al., 2008; Fox et al., 2005; Raichle et al., 2001). Notably, most of the voxels within the posterior IPL

TABLE 5. A COMPARISON BETWEEN THE CURRENT SEVEN CLUSTERS AND SUBDIVISIONS OF THE INFERIOR PARIETAL LOBULE AS IDENTIFIED FROM PREVIOUS WORKS

<i>Our clusters</i>		<i>Mars and colleagues (2011)</i>	<i>Wang and colleagues (2012)</i>
Dorsal-anterior IPL (cluster 3)	PFt ^{a,b} /hIP2 ^c	Blue	Blue
Ventral-anterior IPL (cluster 2)	PFop ^{a,b}	Red	Green
Dorsal anterior-middle IPL (cluster 4)	PF ^{1,2} /PFm ^{a,b}	Green/Blue	Light green
Ventral anterior-middle IPL (cluster 7)	PFcm ^{a,b} /PF ^{a,b}	Green	Yellow
Lateral posterior-middle IPL (cluster 1)	PFm ^{a,b} /PGa ^{a,b}	Green	Orange
Medial posterior-middle IPL (cluster 5)	hIP1 ^c /PGa ^{a,b}	Yellow	Light green/yellow
Posterior IPL (cluster 6)	PGp ^{a,b}	Yellow	Red

^aCaspers and colleagues (2006); ^bCaspers and colleagues (2008); ^cChoi and colleagues (2006); we did not observe a unique cluster that corresponds to PGa. Instead, PGa seems to be related to two clusters, including the lateral posterior-middle IPL (cluster 1, also including the PFm by cytoarchitectonics and close to Mars et al.'s green cluster and Wang et al.'s orange cluster) and medial posterior-middle IPL (cluster 5, also including hIP1 by cytoarchitectonics).

hIP1, human intraparietal area 1; hIP2, human intraparietal area 2.

are located in the posterior AG, confirming a previous report that the DMN is more closely associated with the posterior than anterior AG (Uddin et al., 2010). In contrast, the anterior AG (within cluster 1 and 5) is functionally closer to the middle IPL. These results support functional parcellation of the anterior and posterior AG (Seghier, 2013).

The IPL is known to be involved in the mathematical cognitive processing (Ansari, 2008; Nieder and Dehaene, 2009). The middle IPL, especially cluster 5, responds consistently to mathematical operations (Cohen et al., 2000; Cohen Kadosh et al., 2007; Delazer et al., 2003; Fulbright et al., 2000; Grabner et al., 2009; Kroger et al., 2008; Naccache and Dehaene, 2001; Piazza et al., 2007; Zhang et al., 2012b). On the other hand, the posterior IPL seems involved in the use of learned mathematics, as when comparing trained and untrained conditions (Delazer et al., 2003; Grabner et al., 2009), in contrast to the middle IPL.

The IPL is also critically involved in attention and memory processing (Ciaramelli et al., 2008; Hutchinson et al., 2009; Uncapher and Wagner, 2009). According to the published coordinates, attention and memory primarily engage the middle and posterior IPL (Astafiev et al., 2003; Beauchamp et al., 2001; Connolly et al., 2002; Corbetta et al., 2000; Corbetta and Shulman, 2002; Henson et al., 1999; Hopfinger et al., 2000; Indovina and Macaluso, 2007; Jack et al., 2007; Johnson and Rugg, 2007; Kincade et al., 2005; Macaluso and Patria, 2007; Pessoa et al., 2002; Shulman et al., 2002; Sylvester et al., 2007; Vossel et al., 2006; Wheeler and Buckner, 2004). In an “attention to memory” hypothesis, Cabeza and colleagues proposed two attentional systems, each involving different parts of the IPL. The center of mass of activity for top-down (median coordinates: $x = -36$, $y = -57$, $z = 42$) and bottom-up (median coordinates: $x = -50$, $y = -57$, $z = 38$) attention each corresponds to the middle and posterior IPL (Cabeza et al., 2008; Ciaramelli et al., 2008). Further, a work of Corbetta and Schulman (2002) (Ciaramelli et al., 2008; Corbetta and Shulman, 2002) defined the top-down or dorsal attention network, which includes the superior parietal lobule, frontal eye field, as well as the fusiform and middle temporal gyrus; and the bottom-up or ventral attention network, which includes the temporoparietal junction, inferior and middle frontal gyri, as well as ventrolateral prefrontal gyrus. Our study showed that both middle and posterior IPL connected with the inferior and middle frontal gyri and ventrolateral prefrontal gyrus. However, the superior parietal lobule, key to top-down attention, showed positive connectivity to the middle IPL but negative connectivity to the posterior IPL. Only the middle IPL connected with the fusiform gyrus. Our findings, thus, suggested that the middle and posterior IPL each belongs to the top-down and bottom-up attentional systems. However, there is likely a complex interplay between these IPL subregions in attentional processing.

In contrast, the anterior IPL responds to target compared with baseline conditions in “oddball” visual attention tasks (Bledowski et al., 2004; Braver et al., 2001; Kiehl et al., 2001; Linden et al., 1999; Menon et al., 1997). The anterior IPL connected with the supplementary motor area, primary motor cortex, postcentral gyrus, superior temporal gyrus, putamen, pallidum, as well as insula, areas that respond to targets in oddball tasks (Bledowski et al., 2004; Braver et al., 2001; Kiehl et al., 2001; Linden et al., 1999;

Menon et al., 1997). On the other hand, the middle IPL as well as its connected areas, including the superior, middle, and inferior frontal gyri, and middle cingulate cortex, respond to novel compared with baseline conditions in the oddball paradigms (Bledowski et al., 2004; Braver et al., 2001; Kiehl et al., 2001; Linden et al., 1999; Menon et al., 1997).

Reviewing fMRI studies of memory retrieval and summarizing the coordinates of activation, Vilberg and Rugg noted that the middle and posterior IPL is each more associated with familiarity and recollection-related judgment (Vilberg and Rugg, 2008). Our findings demonstrated that the middle IPL showed connectivity with the superior parietal lobule, parahippocampus, and middle cingulate cortex, known to be involved in familiarity-related judgment (Daselaar et al., 2006; Montaldi et al., 2006; Ragland et al., 2006; Vilberg and Rugg, 2007; Woodruff et al., 2005). In contrast, the posterior IPL showed connectivity with the posterior cingulate cortex, precuneus, and medial prefrontal cortex, known to be involved in recollection-related judgment (Cansino et al., 2002; Daselaar et al., 2006; Eldridge et al., 2000; Fenker et al., 2005; Johnson and Rugg, 2007; Montaldi et al., 2006; Ragland et al., 2006; Vilberg and Rugg, 2007; Woodruff et al., 2005). It should be noted that the latter finding also accords with a role of the DMN in self-related inferential processing.

Taken together, these findings suggested that anterior, middle, and posterior IPL have distinct patterns of resting-state functional connectivity which mirror their roles in attention, memory, and other cognitive processes.

Hemispheric differences in IPL connectivity and functions

The IPL is known for its hemispheric differences in cognitive functions, with the right IPL predominantly involved in spatial attention processing (Cicek et al., 2007; Husain and Nachev, 2007; Singh-Curry and Husain, 2009) and mathematical cognition (Chochon et al., 1999) and the left IPL involved in tool use (Johnson-Frey et al., 2005; Rushworth et al., 2001, 2003) and language and semantic processing (Awad et al., 2007; Brownsett and Wise, 2010; Sharp et al., 2010; Vigneau et al., 2006). In support of these functional differences, right IPL lesion frequently leads to spatial neglect, while left IPL lesion leads to the syndrome of apraxia (De Renzi, 1985; Rushworth et al., 1997; Goldenberg and Karnath, 2006; Husain and Nachev, 2007; Pazzaglia et al., 2008).

In the current study, the left but not right dorsal anterior-middle IPL (cluster 4) showed significant connectivity with the left primary motor cortex, which was consistent with the hemispheric differences of the IPL in the competency of tool use and motor attention (Devlin et al., 2002; Johnson-Frey et al., 2005; Rushworth et al., 2001, 2003). For instance, Rushworth and colleagues (2001, 2003) observed the left but not right IPL (within our cluster 4) activation during motor attention. In a meta-analysis of seven published positron emission tomography studies, Devlin and colleagues (2002) reported activation of the left IPL (within cluster 2) during tool use under a variety of experimental conditions. The left but not right posterior IPL (cluster 6) showed significant connectivity with the left orbital part of the inferior frontal gyrus, the Wernicke’s area, which was consistent with previous findings of hemispheric differences of the

AG in language and semantic processing (Awad et al., 2007; Brownsett and Wise, 2010; Sharp et al., 2010; Vigneau et al., 2006). For instance, the left but not right ventral AG responded meaningfully in contrast to meaningless narrative in a speech task (Brownsett and Wise, 2010).

In contrast, the right but not left IPL is implicated in allocating spatial attention (Cicek et al., 2007; Singh-Curry and Husain, 2009). We observed that the right but not left dorsal anterior-middle IPL (cluster 4) showed connectivity with the right superior frontal gyrus, right orbital part of the inferior frontal gyrus, right insula, and right middle cingulate gyrus; the right but not left dorsal-anterior IPL (cluster 3) showed connectivity with the right triangular part of the inferior frontal gyrus and right middle frontal gyrus, areas known to mediate spatial attention (Casey et al., 2000; Corbetta and Shulman, 2002; Egner et al., 2008; Stevens et al., 2005). More broadly, spatial attention involved greater right-hemispheric activation of the superior frontal gyrus, inferior frontal gyrus, and IPL (Stevens et al., 2005). Our findings were also consistent with the hemispheric differences revealed with probabilistic fiber tract analysis (Caspers et al., 2011) that the rostral IPL areas PFt (close to our cluster 3) and PF (close to our cluster 4) showed more consistent connections with the inferior opercular and orbitofrontal areas and insula in the right than the left hemisphere.

Methodological notes

In addition to positive correlations between functionally related brain regions, negative correlations have also been observed between brain regions with theoretically opposed functional roles (Chen et al., 2011; Fox et al., 2005; Fransson, 2005; Greicius et al., 2003; Uddin et al., 2009). Recent studies suggested that the global signal regression, a common step of data preprocessing in seed region-based functional connectivity analyses, is a likely cause of anti-correlated functional networks (Murphy et al., 2009; Weissenbacher et al., 2009). On the other hand, it has also been demonstrated that the multiple characteristics of anti-correlated networks, including cross-subject consistency, spatial distribution, as well as presence with modified whole-brain masks and before global signal regression, are not determined by global regression (Fox et al., 2009). In our previous study of the medial superior frontal cortex that was based on the same data set, we examined this issue by repeating the same analysis only without global signal regression (Zhang et al., 2012a). The results showed a very similar pattern of functional connectivity as in the analyses with global signal regression, suggesting that the negative connectivities are not a result of image preprocessing.

We used correlations between the IPL voxels and 116 AAL masks instead of thousands of voxels of the entire brain for K-means clustering. There were two advantages. First, it reduced computation load by several orders of magnitude. Second, the averaged time series of a brain region is always more stable than the time series of a single voxel. Therefore, we could have more stable correlations using averaged time series. For instance, the voxels at the edge of the brain may have noisy time series, leading to unusual correlations, which, in turn, compromises K-means clustering. On the other hand, we acknowledge that all the 116 AAL regions

are not functionally homogenous. We may lose information by averaging them.

Potential clinical implications

Structural and functional abnormalities of the IPL were observed in many neurological conditions, including Alzheimer's disease (Greene and Killiany, 2010; Hanggi et al., 2011; Nelson et al., 2009; Neufang et al., 2011; Xia and He, 2011; Zahn et al., 2005) and mild cognitive impairment (Chong and Sahadevan, 2005; Greene and Killiany, 2010; Hamalainen et al., 2007; Hanggi et al., 2011; Liang et al., 2012; Markesbery et al., 2006; Walker and Walker, 2005). For instance, Liang et al. (2012) showed that the AG connectivity with the DMN was significantly reduced in mild cognitive impairment. Another recent study also suggested that the subregions of the IPL were differentially affected in the progression from mild to severe Alzheimer's disease (Greene and Killiany, 2010). Characterizing the functional connectivity of these subregions would further our understanding of the functions of the IPL and shed new lights on how dysfunctions of the IPL may contribute to the clinical manifestations of these neurological processes.

Acknowledgments

This study was supported by NIH grants R01DA023248 (C.-S.R.L.), K02DA026990 (C.-S.R.L.), R21AA018004 (C.-S.R.L.), and P20DA027844 (Potenza). The NIH had no further role in study design; in the collection, analysis, and interpretation of data; in the writing of the report; or in the decision to submit this article for publication. The authors thank investigators of the 1000 Functional Connectomes Project and those who shared the data set for making this study possible.

Author Disclosure Statement

No competing financial interests exist.

References

- Ansari D. 2008. Effects of development and enculturation on number representation in the brain. *Nat Rev Neurosci* 9:278–291.
- Ashburner J, Friston KJ. 1999. Nonlinear spatial normalization using basis functions. *Hum Brain Mapp* 7:254–266.
- Astafiev SV, Shulman GL, Stanley CM, Snyder AZ, Van Essen DC, Corbetta M. 2003. Functional organization of human intraparietal and frontal cortex for attending, looking, and pointing. *J Neurosci* 23:4689–4699.
- Awad M, Warren JE, Scott SK, Turkheimer FE, Wise RJ. 2007. A common system for the comprehension and production of narrative speech. *J Neurosci* 27:11455–11464.
- Barnes KA, Cohen AL, Power JD, Nelson SM, Dosenbach YB, Miezin FM, Petersen SE, Schlaggar BL. 2010. Identifying basal ganglia divisions in individuals using resting-state functional connectivity MRI. *Front Syst Neurosci* 4:18.
- Beauchamp MS, Petit L, Ellmore TM, Ingeholm J, Haxby JV. 2001. A parametric fMRI study of overt and covert shifts of visuospatial attention. *Neuroimage* 14:310–321.
- Berry KJ, Mielke PW, Jr. 2000. A Monte Carlo investigation of the Fisher Z transformation for normal and nonnormal distributions. *Psychol Rep* 87:1101–1114.

- Binder JR, Desai RH, Graves WW, Conant LL. 2009. Where is the semantic system? A critical review and meta-analysis of 120 functional neuroimaging studies. *Cereb Cortex* 19:2767–2796.
- Biswal B, Yetkin FZ, Haughton VM, Hyde JS. 1995. Functional connectivity in the motor cortex of resting human brain using echo-planar MRI. *Magn Reson Med* 34:537–541.
- Biswal BB, Mennes M, Zuo XN, Gohel S, Kelly C, Smith SM, Beckmann CF, Adelstein JS, Buckner RL, Colcombe S, Dogonowski AM, Ernst M, Fair D, Hampson M, Hoptman MJ, Hyde JS, Kiviniemi VJ, Kotter R, Li SJ, Lin CP, Lowe MJ, Mackay C, Madden DJ, Madsen KH, Margulies DS, Mayberg HS, McMahon K, Monk CS, Mostofsky SH, Nagel BJ, Pekar JJ, Peltier SJ, Petersen SE, Riedl V, Rombouts SA, Rypma B, Schlaggar BL, Schmidt S, Seidler RD, Siegle GJ, Sorg C, Teng GJ, Vejjola J, Villringer A, Walter M, Wang L, Weng XC, Whitfield-Gabrieli S, Williamson P, Windischberger C, Zang YF, Zhang HY, Castellanos FX, Milham MP. 2010. Toward discovery science of human brain function. *Proc Natl Acad Sci U S A* 107:4734–4739.
- Bledowski C, Prvulovic D, Goebel R, Zanella FE, Linden DE. 2004. Attentional systems in target and distractor processing: a combined ERP and fMRI study. *Neuroimage* 22:530–540.
- Braver TS, Barch DM, Gray JR, Molfese DL, Snyder A. 2001. Anterior cingulate cortex and response conflict: effects of frequency, inhibition and errors. *Cereb Cortex* 11:825–836.
- Brownsett SL, Wise RJ. 2010. The contribution of the parietal lobes to speaking and writing. *Cereb Cortex* 20:517–523.
- Buckner RL, Andrews-Hanna JR, Schacter DL. 2008. The brain's default network: anatomy, function, and relevance to disease. *Ann N Y Acad Sci* 1124:1–38.
- Cabeza R, Ciaramelli E, Olson IR, Moscovitch M. 2008. The parietal cortex and episodic memory: an attentional account. *Nat Rev Neurosci* 9:613–625.
- Cansino S, Maquet P, Dolan RJ, Rugg MD. 2002. Brain activity underlying encoding and retrieval of source memory. *Cereb Cortex* 12:1048–1056.
- Casey BJ, Thomas KM, Welsh TF, Badgaiyan RD, Eccard CH, Jennings JR, Crone EA. 2000. Dissociation of response conflict, attentional selection, and expectancy with functional magnetic resonance imaging. *Proc Natl Acad Sci U S A* 97:8728–8733.
- Caspers S, Eickhoff SB, Geyer S, Scheperjans F, Mohlberg H, Zilles K, Amunts K. 2008. The human inferior parietal lobule in stereotaxic space. *Brain Struct Funct* 212:481–495.
- Caspers S, Eickhoff SB, Rick T, von Kapri A, Kuhlen T, Huang R, Shah NJ, Zilles K. 2011. Probabilistic fibre tract analysis of cytoarchitectonically defined human inferior parietal lobule areas reveals similarities to macaques. *Neuroimage* 58:362–380.
- Caspers S, Geyer S, Schleicher A, Mohlberg H, Amunts K, Zilles K. 2006. The human inferior parietal cortex: cytoarchitectonic parcellation and interindividual variability. *Neuroimage* 33:430–448.
- Cauda F, Geminiani G, D'Agata F, Sacco K, Duca S, Bagshaw AP, Cavanna AE. 2010. Functional connectivity of the post-eromedial cortex. *PLoS One* 5:e13107.
- Chambers CD, Payne JM, Stokes MG, Mattingley JB. 2004. Fast and slow parietal pathways mediate spatial attention. *Nat Neurosci* 7:217–218.
- Charles F, Bond J, Richardson K. 2004. Seeing the fisher z-transformation. *Psychometrika* 69:291–303.
- Chen G, Chen G, Xie C, Li SJ. 2011. Negative functional connectivity and its dependence on the shortest path length of positive network in the resting-state human brain. *Brain Connect* 1:195–206.
- Chochon F, Cohen L, van de Moortele PF, Dehaene S. 1999. Differential contributions of the left and right inferior parietal lobules to number processing. *J Cogn Neurosci* 11:617–630.
- Choi HJ, Zilles K, Mohlberg H, Schleicher A, Fink GR, Armstrong E, Amunts K. 2006. Cytoarchitectonic identification and probabilistic mapping of two distinct areas within the anterior ventral bank of the human intraparietal sulcus. *J Comp Neurol* 495:53–69.
- Chong MS, Sahadevan S. 2005. Preclinical Alzheimer's disease: diagnosis and prediction of progression. *Lancet Neurol* 4:576–579.
- Chou TL, Booth JR, Bitan T, Burman DD, Bigio JD, Cone NE, Lu D, Cao F. 2006a. Developmental and skill effects on the neural correlates of semantic processing to visually presented words. *Hum Brain Mapp* 27:915–924.
- Chou TL, Booth JR, Burman DD, Bitan T, Bigio JD, Lu D, Cone NE. 2006b. Developmental changes in the neural correlates of semantic processing. *Neuroimage* 29:1141–1149.
- Ciaramelli E, Grady CL, Moscovitch M. 2008. Top-down and bottom-up attention to memory: a hypothesis (AtoM) on the role of the posterior parietal cortex in memory retrieval. *Neuropsychologia* 46:1828–1851.
- Cicek M, Gitelman D, Hurley RS, Nobre A, Mesulam M. 2007. Anatomical physiology of spatial extinction. *Cereb Cortex* 17:2892–2898.
- Claeys KG, Lindsey DT, De Schutter E, Orban GA. 2003. A higher order motion region in human inferior parietal lobule: evidence from fMRI. *Neuron* 40:631–642.
- Clark D, Wagner AD. 2003. Assembling and encoding word representations: fMRI subsequent memory effects implicate a role for phonological control. *Neuropsychologia* 41:304–317.
- Cohen Kadosh R, Cohen Kadosh K, Kaas A, Henik A, Goebel R. 2007. Notation-dependent and -independent representations of numbers in the parietal lobes. *Neuron* 53:307–314.
- Cohen L, Dehaene S, Chochon F, Lehericy S, Naccache L. 2000. Language and calculation within the parietal lobe: a combined cognitive, anatomical and fMRI study. *Neuropsychologia* 38:1426–1440.
- Connolly JD, Goodale MA, Menon RS, Munoz DP. 2002. Human fMRI evidence for the neural correlates of preparatory set. *Nat Neurosci* 5:1345–1352.
- Corbetta M, Kincade JM, Ollinger JM, McAvoy MP, Shulman GL. 2000. Voluntary orienting is dissociated from target detection in human posterior parietal cortex. *Nat Neurosci* 3:292–297.
- Corbetta M, Shulman GL. 2002. Control of goal-directed and stimulus-driven attention in the brain. *Nat Rev Neurosci* 3:201–215.
- Cordes D, Haughton VM, Arfanakis K, Carew JD, Turski PA, Moritz CH, Quigley MA, Meyerand ME. 2001. Frequencies contributing to functional connectivity in the cerebral cortex in “resting-state” data. *AJNR Am J Neuroradiol* 22:1326–1333.
- Daselaar SM, Fleck MS, Cabeza R. 2006. Triple dissociation in the medial temporal lobes: recollection, familiarity, and novelty. *J Neurophysiol* 96:1902–1911.
- Daselaar SM, Prince SE, Cabeza R. 2004. When less means more: deactivations during encoding that predict subsequent memory. *Neuroimage* 23:921–927.

- Davachi L, Maril A, Wagner AD. 2001. When keeping in mind supports later bringing to mind: neural markers of phonological rehearsal predict subsequent remembering. *J Cogn Neurosci* 13:1059–1070.
- De Renzi E. 1985. Methods of limb apraxia examination and their bearing on the interpretation of the disorder. In: Roy EA (ed.) *Neuropsychological Studies of Apraxia and Related Disorders*. Amsterdam, Netherlands: Elsevier; pp. 45–64.
- Dehaene S, Molko N, Cohen L, Wilson AJ. 2004. Arithmetic and the brain. *Curr Opin Neurobiol* 14:218–224.
- Delazer M, Domahs F, Bartha L, Brenneis C, Lochy A, Trieb T, Benke T. 2003. Learning complex arithmetic—an fMRI study. *Brain Res Cogn Brain Res* 18:76–88.
- Devlin JT, Moore CJ, Mummery CJ, Gorno-Tempini ML, Phillips JA, Noppeney U, Frackowiak RS, Friston KJ, Price CJ. 2002. Anatomic constraints on cognitive theories of category specificity. *Neuroimage* 15:675–685.
- Doucet G, Naveau M, Petit L, Delcroix N, Zago L, Crivello F, Jobard G, Tzourio-Mazoyer N, Mazoyer B, Mellet E, Joliot M. 2011. Brain activity at rest: a multiscale hierarchical functional organization. *J Neurophysiol* 105:2753–2763.
- Egner T, Monti JM, Trittschuh EH, Wieneke CA, Hirsch J, Mesulam MM. 2008. Neural integration of top-down spatial and feature-based information in visual search. *J Neurosci* 28:6141–6151.
- Eldridge LL, Knowlton BJ, Furmanski CS, Bookheimer SY, Engel SA. 2000. Remembering episodes: a selective role for the hippocampus during retrieval. *Nat Neurosci* 3:1149–1152.
- Fair DA, Schlaggar BL, Cohen AL, Miezin FM, Dosenbach NU, Wenger KK, Fox MD, Snyder AZ, Raichle ME, Petersen SE. 2007. A method for using blocked and event-related fMRI data to study “resting state” functional connectivity. *Neuroimage* 35:396–405.
- Fenker DB, Schott BH, Richardson-Klavehn A, Heinze HJ, Duzel E. 2005. Recapitulating emotional context: activity of amygdala, hippocampus and fusiform cortex during recollection and familiarity. *Eur J Neurosci* 21:1993–1999.
- Fox MD, Raichle ME. 2007. Spontaneous fluctuations in brain activity observed with functional magnetic resonance imaging. *Nat Rev Neurosci* 8:700–711.
- Fox MD, Snyder AZ, Vincent JL, Corbetta M, Van Essen DC, Raichle ME. 2005. The human brain is intrinsically organized into dynamic, anticorrelated functional networks. *Proc Natl Acad Sci U S A* 102:9673–9678.
- Fox MD, Zhang D, Snyder AZ, Raichle ME. 2009. The global signal and observed anticorrelated resting state brain networks. *J Neurophysiol* 101:3270–3283.
- Fransson P. 2005. Spontaneous low-frequency BOLD signal fluctuations: an fMRI investigation of the resting-state default mode of brain function hypothesis. *Hum Brain Mapp* 26:15–29.
- Friston K, Ashburner J, Frith C, Polone J, Heather J, Frackowiak R. 1995. Spatial registration and normalization of images. *Hum Brain Mapp* 2:165–189.
- Fulbright RK, Molfese DL, Stevens AA, Skudlarski P, Lacadie CM, Gore JC. 2000. Cerebral activation during multiplication: a functional MR imaging study of number processing. *AJNR Am J Neuroradiol* 21:1048–1054.
- Garey LJ. 2006. *Brodman's Localisation in the Cerebral Cortex*. New York: Springer.
- Gentle JE, Härdle W, Mori Y. 2004. *Handbook of Computational Statistics: Concepts and Methods*. Berlin: Springer-Verlag.
- Goldenberg G, Karnath HO. 2006. The neural basis of imitation is body part specific. *J Neurosci* 26:6282–6287.
- Grabner RH, Ischebeck A, Reishofer G, Koschutnig K, Delazer M, Ebner F, Neuper C. 2009. Fact learning in complex arithmetic and figural-spatial tasks: the role of the angular gyrus and its relation to mathematical competence. *Hum Brain Mapp* 30:2936–2952.
- Greene SJ, Killiany RJ. 2010. Subregions of the inferior parietal lobule are affected in the progression to Alzheimer's disease. *Neurobiol Aging* 31:1304–1311.
- Greicius MD, Krasnow B, Reiss AL, Menon V. 2003. Functional connectivity in the resting brain: a network analysis of the default mode hypothesis. *Proc Natl Acad Sci U S A* 100:253–258.
- Hamalainen A, Pihlajamaki M, Tanila H, Hanninen T, Niskanen E, Tervo S, Karjalainen PA, Vanninen RL, Soinen H. 2007. Increased fMRI responses during encoding in mild cognitive impairment. *Neurobiol Aging* 28:1889–1903.
- Hanggi J, Streffer J, Jancke L, Hock C. 2011. Volumes of lateral temporal and parietal structures distinguish between healthy aging, mild cognitive impairment, and Alzheimer's disease. *J Alzheimers Dis* 26:719–734.
- Henson RN, Rugg MD, Shallice T, Josephs O, Dolan RJ. 1999. Recollection and familiarity in recognition memory: an event-related functional magnetic resonance imaging study. *J Neurosci* 19:3962–3972.
- Hopfinger JB, Buonocore MH, Mangun GR. 2000. The neural mechanisms of top-down attentional control. *Nat Neurosci* 3:284–291.
- Husain M, Nachev P. 2007. Space and the parietal cortex. *Trends Cogn Sci* 11:30–36.
- Hutchinson JB, Uncapher MR, Wagner AD. 2009. Posterior parietal cortex and episodic retrieval: convergent and divergent effects of attention and memory. *Learn Mem* 16:343–356.
- Indovina I, Macaluso E. 2007. Dissociation of stimulus relevance and saliency factors during shifts of visuospatial attention. *Cereb Cortex* 17:1701–1711.
- Ishibashi R, Lambon Ralph MA, Saito S, Pobric G. 2011. Different roles of lateral anterior temporal lobe and inferior parietal lobule in coding function and manipulation tool knowledge: evidence from an rTMS study. *Neuropsychologia* 49:1128–1135.
- Jack AI, Patel GH, Astafiev SV, Snyder AZ, Akbudak E, Shulman GL, Corbetta M. 2007. Changing human visual field organization from early visual to extra-occipital cortex. *PLoS One* 2:e452.
- Jenkins GM, Watts DG. 1968. *Spectral Analysis and Its Applications*. San Francisco, CA: Holden-Day.
- Johnson-Frey SH, Newman-Norlund R, Grafton ST. 2005. A distributed left hemisphere network active during planning of everyday tool use skills. *Cereb Cortex* 15:681–695.
- Johnson JD, Rugg MD. 2007. Recollection and the reinstatement of encoding-related cortical activity. *Cereb Cortex* 17:2507–2515.
- Kahnt T, Chang LJ, Park SQ, Heinzle J, Haynes JD. 2012. Connectivity-based parcellation of the human orbitofrontal cortex. *J Neurosci* 32:6240–6250.
- Kiehl KA, Laurens KR, Duty TL, Forster BB, Liddle PF. 2001. Neural sources involved in auditory target detection and novelty processing: an event-related fMRI study. *Psychophysiology* 38:133–142.
- Kim JH, Lee JM, Jo HJ, Kim SH, Lee JH, Kim ST, Seo SW, Cox RW, Na DL, Kim SI, Saad ZS. 2010. Defining functional SMA and pre-SMA subregions in human MFC using resting state fMRI: functional connectivity-based parcellation method. *Neuroimage* 49:2375–2386.

- Kincade JM, Abrams RA, Astafiev SV, Shulman GL, Corbetta M. 2005. An event-related functional magnetic resonance imaging study of voluntary and stimulus-driven orienting of attention. *J Neurosci* 25:4593–4604.
- Kroger JK, Nystrom LE, Cohen JD, Johnson-Laird PN. 2008. Distinct neural substrates for deductive and mathematical processing. *Brain Res* 1243:86–103.
- Liang P, Wang Z, Yang Y, Li K. 2012. Three subsystems of the inferior parietal cortex are differently affected in mild cognitive impairment. *J Alzheimers Dis* 30:475–487.
- Linden DE, Prvulovic D, Formisano E, Vollinger M, Zanella FE, Goebel R, Dierks T. 1999. The functional neuroanatomy of target detection: an fMRI study of visual and auditory oddball tasks. *Cereb Cortex* 9:815–823.
- Lowe MJ, Mock BJ, Sorenson JA. 1998. Functional connectivity in single and multislice echoplanar imaging using resting-state fluctuations. *Neuroimage* 7:119–132.
- Macaluso E, Patria F. 2007. Spatial re-orienting of visual attention along the horizontal or the vertical axis. *Exp Brain Res* 180:23–34.
- MacQueen JB. 1967. Some methods for classification and analysis of multivariate observations. In: *5-th Berkeley Symposium on Mathematical Statistics and Probability*, vol. 1. Berkeley, CA: University of California Press; pp. 281–297.
- Margulies DS, Kelly AM, Uddin LQ, Biswal BB, Castellanos FX, Milham MP. 2007. Mapping the functional connectivity of anterior cingulate cortex. *Neuroimage* 37:579–588.
- Margulies DS, Vincent JL, Kelly C, Lohmann G, Uddin LQ, Biswal BB, Villringer A, Castellanos FX, Milham MP, Petrides M. 2009. Precuneus shares intrinsic functional architecture in humans and monkeys. *Proc Natl Acad Sci U S A* 106:20069–20074.
- Markesbery WR, Schmitt FA, Kryscio RJ, Davis DG, Smith CD, Wekstein DR. 2006. Neuropathologic substrate of mild cognitive impairment. *Arch Neurol* 63:38–46.
- Mars RB, Jbabdi S, Sallet J, O'Reilly JX, Croxson PL, Olivier E, Noonan MP, Bergmann C, Mitchell AS, Baxter MG, Behrens TE, Johansen-Berg H, Tomassini V, Miller KL, Rushworth MF. 2011. Diffusion-weighted imaging tractography-based parcellation of the human parietal cortex and comparison with human and macaque resting-state functional connectivity. *J Neurosci* 31:4087–4100.
- Martinez-Trujillo JC, Cheyne D, Gaetz W, Simine E, Tsotsos JK. 2007. Activation of area MT/V5 and the right inferior parietal cortex during the discrimination of transient direction changes in translational motion. *Cereb Cortex* 17:1733–1739.
- Mayer AR, Harrington D, Adair JC, Lee R. 2006. The neural networks underlying endogenous auditory covert orienting and reorienting. *Neuroimage* 30:938–949.
- Menon V, Ford JM, Lim KO, Glover GH, Pfefferbaum A. 1997. Combined event-related fMRI and EEG evidence for temporal-parietal cortex activation during target detection. *Neuroreport* 8:3029–3037.
- Montaldi D, Spencer TJ, Roberts N, Mayes AR. 2006. The neural system that mediates familiarity memory. *Hippocampus* 16:504–520.
- Murphy K, Birn RM, Handwerker DA, Jones TB, Bandettini PA. 2009. The impact of global signal regression on resting state correlations: are anti-correlated networks introduced? *Neuroimage* 44:893–905.
- Naccache L, Dehaene S. 2001. The priming method: imaging unconscious repetition priming reveals an abstract representation of number in the parietal lobes. *Cereb Cortex* 11:966–974.
- Nelson PT, Abner EL, Scheff SW, Schmitt FA, Kryscio RJ, Jicha GA, Smith CD, Patel E, Markesbery WR. 2009. Alzheimer's-type neuropathology in the precuneus is not increased relative to other areas of neocortex across a range of cognitive impairment. *Neurosci Lett* 450:336–339.
- Nelson SM, Cohen AL, Power JD, Wig GS, Miezin FM, Wheeler ME, Velanova K, Donaldson DI, Phillips JS, Schlaggar BL, Petersen SE. 2010. A parcellation scheme for human left lateral parietal cortex. *Neuron* 67:156–170.
- Neufang S, Akhrif A, Riedl V, Forstl H, Kurz A, Zimmer C, Sorg C, Wohlschlagger AM. 2011. Disconnection of frontal and parietal areas contributes to impaired attention in very early Alzheimer's disease. *J Alzheimers Dis* 25:309–321.
- Nieder A, Dehaene S. 2009. Representation of number in the brain. *Annu Rev Neurosci* 32:185–208.
- O'Reilly JX, Beckmann CF, Tomassini V, Ramnani N, Johansen-Berg H. 2010. Distinct and overlapping functional zones in the cerebellum defined by resting state functional connectivity. *Cereb Cortex* 20:953–965.
- Otten LJ, Rugg MD. 2001. When more means less: neural activity related to unsuccessful memory encoding. *Curr Biol* 11:1528–1530.
- Passingham RE, Stephan KE, Kotter R. 2002. The anatomical basis of functional localization in the cortex. *Nat Rev Neurosci* 3:606–616.
- Pazzaglia M, Smania N, Corato E, Aglioti SM. 2008. Neural underpinnings of gesture discrimination in patients with limb apraxia. *J Neurosci* 28:3030–3041.
- Peeters R, Simone L, Nelissen K, Fabbri-Destro M, Vanduffel W, Rizzolatti G, Orban GA. 2009. The representation of tool use in humans and monkeys: common and uniquely human features. *J Neurosci* 29:11523–11539.
- Penny WD, Holmes AP, Friston K. 2004. Random-effects analysis. In: Frackowiak R, et al. (eds.) *Human Brain Function*. San Diego, CA: Academic Press; pp. 843–850.
- Pessoa L, Gutierrez E, Bandettini P, Ungerleider L. 2002. Neural correlates of visual working memory: fMRI amplitude predicts task performance. *Neuron* 35:975–987.
- Piazza M, Pinel P, Le Bihan D, Dehaene S. 2007. A magnitude code common to numerosities and number symbols in human intraparietal cortex. *Neuron* 53:293–305.
- Power JD, Cohen AL, Nelson SM, Wig GS, Barnes KA, Church JA, Vogel AC, Laumann TO, Miezin FM, Schlaggar BL, Petersen SE. 2011. Functional network organization of the human brain. *Neuron* 72:665–678.
- Ragland JD, Valdez JN, Loughhead J, Gur RC, Gur RE. 2006. Functional magnetic resonance imaging of internal source monitoring in schizophrenia: recognition with and without recollection. *Schizophr Res* 87:160–171.
- Raichle ME, MacLeod AM, Snyder AZ, Powers WJ, Gusnard DA, Shulman GL. 2001. A default mode of brain function. *Proc Natl Acad Sci U S A* 98:676–682.
- Raposo A, Moss HE, Stamatakis EA, Tyler LK. 2006. Repetition suppression and semantic enhancement: an investigation of the neural correlates of priming. *Neuropsychologia* 44:2284–2295.
- Rombouts SA, Stam CJ, Kuijper JP, Scheltens P, Barkhof F. 2003. Identifying confounds to increase specificity during a “no task condition”. Evidence for hippocampal connectivity using fMRI. *Neuroimage* 20:1236–1245.

- Rushworth MF, Behrens TE, Johansen-Berg H. 2006. Connection patterns distinguish 3 regions of human parietal cortex. *Cereb Cortex* 16:1418–1430.
- Rushworth MF, Johansen-Berg H, Gobel SM, Devlin JT. 2003. The left parietal and premotor cortices: motor attention and selection. *Neuroimage* 20 Suppl 1:S89–S100.
- Rushworth MF, Krams M, Passingham RE. 2001. The attentional role of the left parietal cortex: the distinct lateralization and localization of motor attention in the human brain. *J Cogn Neurosci* 13:698–710.
- Rushworth MF, Nixon PD, Renowden S, Wade DT, Passingham RE. 1997. The left parietal cortex and motor attention. *Neuropsychologia* 35:1261–1273.
- Scheperjans F, Eickhoff SB, Homke L, Mohlberg H, Hermann K, Amunts K, Zilles K. 2008a. Probabilistic maps, morphometry, and variability of cytoarchitectonic areas in the human superior parietal cortex. *Cereb Cortex* 18:2141–2157.
- Scheperjans F, Hermann K, Eickhoff SB, Amunts K, Schleicher A, Zilles K. 2008b. Observer-independent cytoarchitectonic mapping of the human superior parietal cortex. *Cereb Cortex* 18:846–867.
- Schmahmann JD, Doyon J, McDonald D, Holmes C, Lavoie K, Hurwitz AS, Kabani N, Toga A, Evans A, Petrides M. 1999. Three-dimensional MRI atlas of the human cerebellum in proportional stereotaxic space. *Neuroimage* 10:233–260.
- Schmahmann JD, Doyon J, Toga A, Petrides M, Evans A. 2000. *MRI Atlas of the Human Cerebellum*. San Diego, CA: Academic Press.
- Schwarz G. 1978. Estimating the dimension of a model. *Ann Stat* 6:461–464.
- Seghier ML. 2013. The angular gyrus: multiple functions and multiple subdivisions. *Neuroscientist* 19:43–61.
- Sharp DJ, Awad M, Warren JE, Wise RJ, Vigliocco G, Scott SK. 2010. The neural response to changing semantic and perceptual complexity during language processing. *Hum Brain Mapp* 31:365–377.
- Shulman GL, d'Avossa G, Tansy AP, Corbetta M. 2002. Two attentional processes in the parietal lobe. *Cereb Cortex* 12:1124–1131.
- Singh-Curry V, Husain M. 2009. The functional role of the inferior parietal lobe in the dorsal and ventral stream dichotomy. *Neuropsychologia* 47:1434–1448.
- Sommer T, Rose M, Buchel C. 2006. Dissociable parietal systems for primacy and subsequent memory effects. *Neurobiol Learn Mem* 85:243–251.
- Stevens MC, Calhoun VD, Kiehl KA. 2005. Hemispheric differences in hemodynamics elicited by auditory oddball stimuli. *Neuroimage* 26:782–792.
- Sylvester CM, Shulman GL, Jack AI, Corbetta M. 2007. Asymmetry of anticipatory activity in visual cortex predicts the locus of attention and perception. *J Neurosci* 27:14424–14433.
- Tzourio-Mazoyer N, Landeau B, Papathanassiou D, Crivello F, Etard O, Delcroix N, Mazoyer B, Joliot M. 2002. Automated anatomical labeling of activations in SPM using a macroscopic anatomical parcellation of the MNI MRI single-subject brain. *Neuroimage* 15:273–289.
- Uddin LQ, Kelly AM, Biswal BB, Xavier Castellanos F, Milham MP. 2009. Functional connectivity of default mode network components: correlation, anticorrelation, and causality. *Hum Brain Mapp* 30:625–637.
- Uddin LQ, Supekar K, Amin H, Rykhlevskaia E, Nguyen DA, Greicius MD, Menon V. 2010. Dissociable connectivity within human angular gyrus and intraparietal sulcus: evidence from functional and structural connectivity. *Cereb Cortex* 20:2636–2646.
- Uncapher MR, Wagner AD. 2009. Posterior parietal cortex and episodic encoding: insights from fMRI subsequent memory effects and dual-attention theory. *Neurobiol Learn Mem* 91:139–154.
- Vigneau M, Beaucoisin V, Herve PY, Duffau H, Crivello F, Houde O, Mazoyer B, Tzourio-Mazoyer N. 2006. Meta-analyzing left hemisphere language areas: phonology, semantics, and sentence processing. *Neuroimage* 30:1414–1432.
- Vilberg KL, Rugg MD. 2007. Dissociation of the neural correlates of recognition memory according to familiarity, recollection, and amount of recollected information. *Neuropsychologia* 45:2216–2225.
- Vilberg KL, Rugg MD. 2008. Memory retrieval and the parietal cortex: a review of evidence from a dual-process perspective. *Neuropsychologia* 46:1787–1799.
- Vossel S, Thiel CM, Fink GR. 2006. Cue validity modulates the neural correlates of covert endogenous orienting of attention in parietal and frontal cortex. *Neuroimage* 32:1257–1264.
- Wagner AD, Davachi L. 2001. Cognitive neuroscience: forgetting of things past. *Curr Biol* 11:R964–R967.
- Walker Z, Walker RW. 2005. Imaging in neurodegenerative disorders: recent studies. *Curr Opin Psychiatry* 18:640–646.
- Wang J, Fan L, Zhang Y, Liu Y, Jiang D, Zhang Y, Yu C, Jiang T. 2012. Tractography-based parcellation of the human left inferior parietal lobule. *Neuroimage* 63:641–652.
- Weissenbacher A, Kasess C, Gerstl F, Lanzenberger R, Moser E, Windischberger C. 2009. Correlations and anticorrelations in resting-state functional connectivity MRI: a quantitative comparison of preprocessing strategies. *Neuroimage* 47:1408–1416.
- Wheeler ME, Buckner RL. 2004. Functional-anatomic correlates of remembering and knowing. *Neuroimage* 21:1337–1349.
- Woodruff CC, Johnson JD, Uncapher MR, Rugg MD. 2005. Content-specificity of the neural correlates of recollection. *Neuropsychologia* 43:1022–1032.
- Xia M, He Y. 2011. Magnetic resonance imaging and graph theoretical analysis of complex brain networks in neuropsychiatric disorders. *Brain Connect* 1:349–365.
- Xu Y, Chun MM. 2009. Selecting and perceiving multiple visual objects. *Trends Cogn Sci* 13:167–174.
- Yeo BT, Krienen FM, Sepulcre J, Sabuncu MR, Lashkari D, Hollinshead M, Roffman JL, Smoller JW, Zollei L, Polimeni JR, Fischl B, Liu H, Buckner RL. 2011. The organization of the human cerebral cortex estimated by intrinsic functional connectivity. *J Neurophysiol* 106:1125–1165.
- Zahn R, Buechert M, Overmans J, Talazko J, Specht K, Ko CW, Thiel T, Kaufmann R, Dykieriek P, Juengling F, Hull M. 2005. Mapping of temporal and parietal cortex in progressive nonfluent aphasia and Alzheimer's disease using chemical shift imaging, voxel-based morphometry and positron emission tomography. *Psychiatry Res* 140:115–131.
- Zhang D, Snyder AZ, Fox MD, Sansbury MW, Shimony JS, Raichle ME. 2008. Intrinsic functional relations between human cerebral cortex and thalamus. *J Neurophysiol* 100:1740–1748.
- Zhang D, Snyder AZ, Shimony JS, Fox MD, Raichle ME. 2010. Noninvasive functional and structural connectivity mapping of the human thalamocortical system. *Cereb Cortex* 20:1187–1194.

- Zhang H, Chen C, Zhou X. 2012b. Neural correlates of numbers and mathematical terms. *Neuroimage* 60:230–240.
- Zhang S, Ide JS, Li CS. 2012a. Resting-state functional connectivity of the medial superior frontal cortex. *Cereb Cortex* 22:99–111.
- Zhang S, Li CS. 2012. Functional connectivity mapping of the human precuneus by resting state fMRI. *Neuroimage* 59: 3548–3562.

Address correspondence to:
Sheng Zhang
Connecticut Mental Health Center S103
34 Park Street
New Haven, CT 06519
E-mail: sheng.zhang@yale.edu